Crystallization-assisted asymmetric synthesis of enantiopure amines using membrane-immobilized transaminase

Hippolyte Meersseman Arango,[a] Neal Bachus,[a] Xuan Dieu Linh Nguyen,[a] Basile Bredun,[a] Patricia Luis,[b] Tom Leyssens,[a] David Roura Padrosa,[c] Francesca Paradisi,[c] Damien P. Debecker[a,*]

[a] Institute of Condensed Matter and Nanosciences (IMCN), Université catholique de Louvain (UCLouvain), Place Louis Pasteur, 1, 1348 Louvain-La-Neuve, Belgium

[b] Materials & Process Engineering (iMMC-IMAP), Université catholique de Louvain, Place Sainte Barbe 2, 1348 Louvain-la-Neuve, Belgium

[c] Department of Chemistry and Biochemistry, University of Bern, Freiestrasse 3, Bern, Switzerland

* damien.debecker@uclouvain.be

ABSTRACT

The production of active pharmaceutical ingredients (APIs) requires enantiopure chiral amines, for which greener synthesis processes are needed. Transaminases (TAs) are enzymes that catalyze the enantioselective production of chiral amines from prochiral ketones, through transamination in mild conditions. Yet, industrial applications of biocatalytic transamination remain currently hindered by the limited stability of soluble enzymes and by the unfavorable thermodynamic equilibrium of targeted asymmetric reactions. Enzyme immobilization can be applied to address stability, recoverability, and reusability issues. In the perspective of process intensification, we chose to immobilize TAs on polymeric (polypropylene) membranes. In the asymmetric synthesis of (R)-2-fluoro-α-methylbenzylamine ((R)-FMBA), such membrane-immobilized TAs exhibited superior specific activity and stability compared to soluble TAs; they also outperformed TAs immobilized on resins. The reaction yield remained, however, limited by thermodynamics. To further enhance the synthesis yield, the reaction was coupled with the *in-situ* crystallization of (R)-FMBA with 3,3-diphenylpropionic acid (DPPA). By doing so, the theoretical equilibrium conversion was pushed from ~44% to ~83%. In fact, a 72 % overall recovery yield of crystallized (R)-FMBA was demonstrated. The enantioselectivity of the reaction was preserved. Importantly, purification was greatly facilitated, since the target enantiopure amine was readily recovered as high purity (R)-FMBA:DPPA crystals. The biocatalytic membranes were found fully reusable, performing successive high-yield asymmetric syntheses with only minor deactivation. Overall, the crystallization-assisted strategy proposed herein offers a greener path for the biocatalytic production of valuable chiral targets.

Keywords: Biocatalysis, immobilized enzymes, chiral amines, crystallization, membranes, process intensification

1 Introduction

Enantiopure amines represent crucial building blocks for the pharmaceutical industry, as they end up in approximately half of the current commercial active pharmaceutical ingredients (API) [1–3]. There is a growing interest for synthesis methods of enantiopure amines that better align with sustainable catalysis practices [4,5]. Amine transaminases (TAs), are increasingly considered as potent biocatalysts for such purpose [6–15]. TAs catalyse the direct synthesis of chiral amines from pro-chiral ketones with excellent enantioselectivity under mild conditions, using inexpensive amino donors through transamination reactions. Despite the impressive deployment of TAs in the scholarly literature, their industrial applications remain limited, as they face two major challenges [9]. On the one hand, TAs employed as free enzymes (soluble) display limited stability and poor recyclability, even when working in mild operating conditions. On the second hand, TAs tend to suffer from substrate/product inhibitions, and most industrially relevant transaminations feature unfavourable thermodynamics [16]. Thus, efforts are underway to enhance the TAs robustness and develop strategies to shift the transamination equilibrium towards the product side.

Enzyme immobilization has proven effective in creating heterogeneous biocatalysts that are more versatile and amenable to more productive processes (e.g. continuous flow) [3,17–22]. Polymeric membranes are available and relatively cheap supports to immobilize biocatalysts (50 €/m^2 can be estimated for membrane contactors [15,23,24], comparable to other materials classically employed for enzyme immobilization purposes, e.g. epoxy-resins from ReliZyme [25,26]). Membrane materials typically offer high surface-to-volume ratios when implemented as modules. Enzyme immobilization on polymeric membranes is now well-documented [27], and the TA membrane-immobilization has been demonstrated [28]. In the literature, researchers have already implemented membrane contactors as downstream processing to purify the transamination products [29–31]. However, immobilizing enzymes on membrane supports could be of further interest, as it additionally offers the possibility to perform biocatalytic reactions along with membrane separation, in a one-pot fashion. For example, the removal of a product could favorably shift the biocatalytic reaction equilibrium toward product formation and mitigate inhibition issues (e.g. acetone removal via pervaporation [32]), and hence increase the reaction rate and final yield. In the specific case of equilibrated transamination reactions, this aspect is of great relevance.

Building up on this aspect, different *in-situ* (co)product removal (ISPR) strategies have been applied to drive transamination reactions towards the products side, such as product extraction (using organic co-solvent or a membrane module), capture/absorption (using ion-exchange resins) and crystallization [15,31,33–37]. Among these product separation strategies, crystallization of the target enantiopure amine product seems particularly suited for the pharmaceutical industry, owing to the high selectivity and high (enantio)purity that can be generally obtained [38,39]. Moreover, it enables the straightforward recovery of the API via simple filtration [40]. von Langermann *et al.* [36], recently disclosed a crystallization-assisted transamination process for the gram-scale preparation of S-(3-methoxyphenyl)ethylamine, a precursor of Rivastigmine. The *in-situ* product crystallization strategy relied on the use of 3,3-diphenylpropionic acid (DPPA), which is able to form poorly soluble crystalline salts with amine compounds [34]. It enabled the production of a pure enantiopure amine product at high concentration (> 1 M) and its straightforward recovery via filtration, and was found applicable to a wide variety of amine targets [41].

In essence, enzyme-membrane reactors coupled with product crystallization can pave the way to greener and intensified chiral amine synthesis processes. Here, we demonstrate the proof of concept of a crystallization-assisted transamination using a membrane-immobilized TA. Polypropylene (PP) was employed as model polymeric membrane to immobilize TAs. An industrially relevant transamination reaction was targeted, i.e. the asymmetric synthesis of (R)-2-fluoro-α-methylbenzylamine ((R)-FMBA) from 2'-fluoroacetophenone (using isopropylamine as amino donor). (R)-FMBA is a precursor of valuable fluorinated chiral *N*-arylamines [42], and its separation is not straightforward (i.e. liquid at room temperature). To the best of our knowledge, such amine building block is not commercially available in its enantiopure form. We show that using a membrane-immobilized TA, in presence of DPPA, allowed reaching yields of pure FMBA:DPPA crystals markedly surpassing the equilibrium yield of the non-assisted reaction. The biocatalytic membrane was also stable and reusable, showing only minor deactivation upon recycling.

2 Experimental

2.1 Materials

Hydrochloric acid (37 wt %, aqueous solution), pyridoxal 5'-phosphate hydrate (PLP; ≥ 98 %), glycerol diglycidyl ether (GDE; technical grade), carbonate-bicarbonate buffer capsules,

Bradford reagent were purchased from Sigma-Aldrich. Sodium hydroxide (NaOH; ≥ 99 %), N-2-Hydroxyethylpiperazine-N'-2-ethane sulphonic acid (HEPES; ≥ 99.5 %), HEPES sodium salt (≥ 99 %) were purchased from Carl Roth. Branched polyethyleneimine (PEI; 50 wt %, aqueous solution, M.N. 60,000), isopropylamine (ISO; 99 %) were purchased from Acros Organics. Dichloromethane (DCM; HPLC grade), ethanol absolute (EtOH), dimethylformamide (DMF; ≥ 99.9 %) were purchased from VWR Chemicals. Tris(hydroxymethyl)aminomethane (Tris; > 99 %), 3-hydroxytyramine hydrochloride (dopamine hydrochloride; 98 %), tert-butyl methyl ether (MTBE; > 99 %), 3,3-diphenylpropionic acid (3-DPPA; 97 %), isopropyl alcohol (iPOH; 99.5 %), tert-butyl alcohol (tBuOH; > 99 %), 2'-fluoroacetophenone (FAP; 97 %), acetophenone (AP, 97 %) were purchased from Tokio Chemical Industry. Methanol (MeOH; 99.8 %) was purchased from Thermo scientific. 2-fluoro-α-methylbenzylamine (FMBA; 97%) was purchased from BLD Pharm. Commercial polypropylene membranes (PP) were purchased from 3M (USA).

Transaminases HeWT (from *Halomonas elongata*) and TsRTA (from *Thermomyces stellatus*) were expressed and lyophilized as previously described by Paradisi et al. [43,44], and then used as cell-free extracts. In some cases, the enzymes were also purified by immobilized metal affinity chromatography (IMAC) in order to be used as pure enzymes (pTA). Distilled water was applied for all synthesis and treatment processes.

2.2 Transaminase immobilization

In this work, the transaminase from *Thermomyces stellatus* (TsRTA) was immobilized onto solid functionalized polypropylene membranes and on ReliZymes resin to run the subsequent heterogeneous transaminations.

2.2.1 Polypropylene membrane (PP)

Polypropylene (PP) membrane surface was functionalized prior to immobilization in order to enable the covalent grafting of TAs, following the method described in details in our previous study [45]. Details and experimental protocols related to these PP functionalization steps are fully described in the electronic supplementary information (ESI). Briefly, it consisted in the successive modifications of a PP membrane with polydopamine (PDA), glycerol diglycidyl ether (GDE) and polyethyleneimine (PEI), separated by intermittent rinsing steps (Figure S1).

A disk of 7 cm^2 (c.a. 35 mg) functionalized PP membrane was immersed into 7.5 mL of buffered solution (HEPES 0.1 M buffer, PLP 1 mM) containing the desired TA concentration

(C_0 = 1 mg.mL^{-1}) at pH 8, and incubated for 18 hours at 35 °C under gentle stirring. After immobilization, the resulting membrane-immobilized transaminase was rinsed with 7.5 mL of rinsing solution (containing PLP 1 mM in HEPES 0.1 M buffer pH 8) for 30 minutes (repeated two times) to eliminate the loosely attached TAs. The immobilization and washing steps were carried out in 10 mL round bottom glass flasks. The heterogeneous biocatalysts obtained upon immobilization of TA cell-free extract (cfe) and pure TA (pTA) were denoted TA_PP and pTA_PP, respectively.

In a variation of this protocol, we also attempted to prepare "self-sufficient" biocatalysts (i.e. not requiring external addition of co-factor during reaction). Inspired by López-Gallego *et al.* [46], we immobilized the TA cfe (using 1 mg.mL^{-1} into 0.1 mM PLP in HEPES 0.1 M buffer pH 8) onto a disk of 7 cm^2 functionalized PP, then rinsed the resulting membrane three time (with 7.5 mL HEPES 0.1 M buffer pH 8, 30 minutes), and directly incubated it with PLP (1 mM in HEPES 10 mM pH 8 for 90 minutes at room temperature under gentle stirring). Additional rinsing was applied again (four times 7.5 mL of HEPES 0.1 M buffer pH 8, 30 minutes). The obtained membrane was denoted TA_PP_SS, where "SS" stands for self-sufficient.

The enzyme loading was evaluated by mass balance, using Bradford titration (see ESI) on the fresh enzyme solutions and on the rinsing solutions.

2.2.2 Benchmark carriers – ReliZymes

For comparison, TA immobilization was also performed in on epoxy-resins (ReliZymeEP and ReliZymeHFA), which are the ubiquitous support materials to immobilize enzymes. 35 mg of epoxy-resin was immersed into 7.5 mL of buffered solution (HEPES 0.1 M buffer, PLP 1 mM) containing the desired TA concentration (C_0 = 1 mg.mL^{-1}) at pH 8, and incubated for 18 hours at 35 °C under gentle shaking. After immobilization, the resulting immobilized transaminase was separated by centrifugation (5 minutes at 14,000 rpm in a Heraeus MultifugeX1R Centrifuge) and rinsed with 7.5 mL of rinsing solution (containing PLP 1 mM in HEPES 0.1 M buffer pH 8) for 30 minutes under gentle shaking (repeated two times) to eliminate the loosely attached TAs. The immobilization and washing steps were carried out in 15 mL Falcon tubes. The resulting benchmark heterogeneous biocatalysts were labelled TA_ReliZymeEP and TA_ReliZymeHFA, depending on the employed epoxy-resin.

2.3 Immobilized enzyme loading evaluation

The immobilized enzyme loading (L) (i.e. the mass of enzyme loaded on the support) was evaluated by mass balance via Eq. 1., using Bradford titration (see section 1 of the ESI). C_0 and C_1 stand for the TA immobilization solution and the residual solution (i.e. obtained after immobilization) respectively, while C_3 and C_4 stand for the first and second rinsing solutions.

$$L = V_0 \times (C_0 - C_1 - C_2 - C_3 - C_4) \ [mg] \qquad \boldsymbol{Eq.1}$$

The immobilization yield (%) is defined as the ratio between immobilized TA (L) and the total TA mass introduced during the immobilization (7.5 x C_0).

2.4 Asymmetric synthesis of (R)-2-fluoro-α-methylbenzylamine ((R)-FMBA)

The asymmetric synthesis of (R)-2-fluoromethylbenzylamine ((R)-FMBA), was carried out in batch mode, using free or immobilized transaminases in batch mode. 2'-fluoroacetophenone (FAP, 10-50 mM) was employed as the amino-acceptor. In order to shift the transamination equilibrium, the reaction was run with an excess of isopropylamine (ISO). Typically, HEPES and PLP were dissolved in distilled water to obtain HEPES 0.1 M, PLP 1 mM solution. ISO (125-500 mM) was then added and the pH was adjusted to pH 8 (using HCl 37 %). TsRTA enzyme (either free or immobilized (as (p)TA_PP, TA_PP_SS, TA_ReliZymeEP or TA_ReliZymeHFA)) was then added in the solution. Then, FAP was added to start the biocatalytic reaction. Reactions were typically run at 35 °C in 7.5 mL total volume (with 10 vol.% methanol), in a 10 mL round bottom glass flask under moderate magnetic stirring.

In some cases, 3,3-diphenylpropionic acid (DPPA) was added (concomitantly with the ISO addition) to crystallize the produced (R)-FMBA in the form of crystal salts to shift the transamination equilibrium (Figure 1). The crystals obtained at the end of reaction were recovered by filtration, rinsed two times with 7.5 mL of HEPES 0.1M buffer, then once with methyl tert-butyl ether (MTBE). Crystals were then dried overnight before further analyses (NMR, chiral-HPLC, pXRD, TGA, see ESI). They were labelled as FMBA:DPPA (x:y), where x and y correspond to the initial FAP and DPPA concentrations. The FMBA:DPPA crystals recovery yield (Y_{cryst}) was defined by Eq. 2 as the ratio of the actual mass of FMBA:DPPA in the obtained crystals ($m_{FMBA:DPPAobt}$) compared to the maximum theoretical mass of FMBA:DPPA produced which is able to crystallize. $[FMBA]_{prod}$ stands for the concentration of FMBA obtained at the end of the biocatalytic test, while s_{FMBA} is the molar solubility of

FMBA in the given reaction medium. $Mw_{FMBA:DPPA}$ stands for the molecular weight of the FMBA:DPPA crystal.

$$Y_{cryst}\ (\%) = \left(\frac{m\ FMBA{:}\ DPPA_{obt}}{\left([FMBA]_{prod} - s_{FMBA}\right) * Mw_{FMBA:DPPA} * V}\right) * 100 \qquad \textbf{\textit{Eq.}\ 2}$$

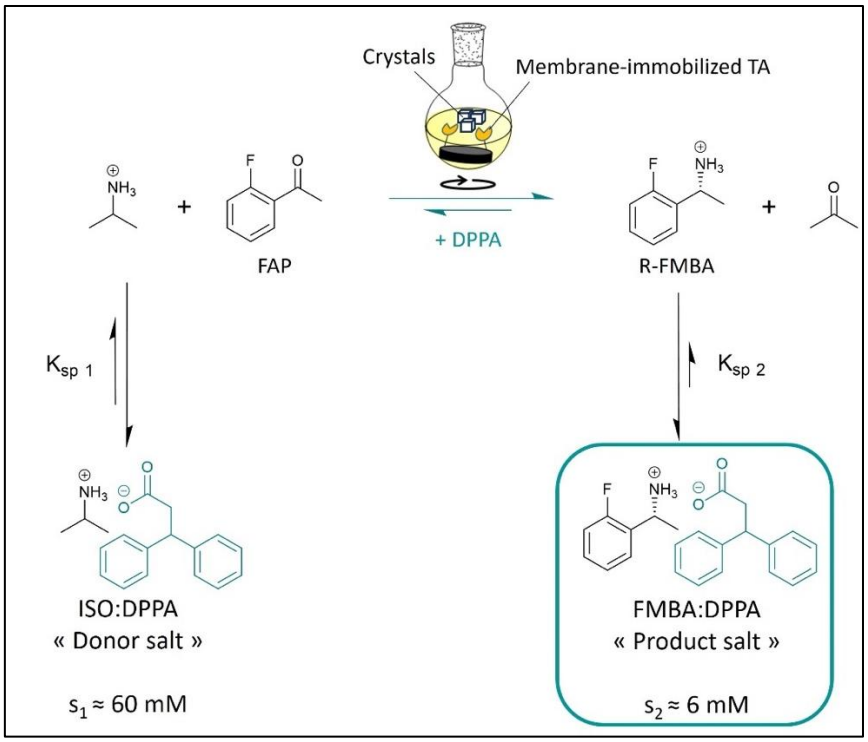

Figure 1. Schematic representation of the targeted heterogeneous asymmetric synthesis of (R)-2-fluoro-α-methylbenzylamine ((R)-FMBA) assisted by product crystallization, using membrane-immobilized TsRTA. Upon addition of 3,3-diphenylpropionic acid (DPPA) in the reaction medium, a donor crystal salt (of molar solubility and solubility product s_1 and Ksp_1, respectively) is formed. As soon as transamination takes place, the produced (R)-FMBA is continuously removed from the medium through the formation of a product crystal salt (of molar solubility and solubility product s_2 and Ksp_2, respectively), thereby shifting the equilibrium towards the product side.

Reaction was followed by analyzing 100 µL samples from the reaction medium. 30 µL of sodium hydroxide (2 M) was added to dissolve the crystal salts, and the mixture was vortexed for 5 seconds. 400 µL of dichloromethane was then added to the aqueous phase, vortexed for 15 seconds and rest for 5 minutes to allow extraction of reactants (ISO, FAP) and products (FMBA, acetone) into the organic phase. Extraction was repeated twice and the organic phases were pooled and analyzed by gas chromatography (see section 1 of the ESI). The specific activity is defined as the number of µmol of 2'-fluoroacetophenone converted per minute per

mg of enzyme. It was evaluated by Eq. 3, where L is the immobilized enzyme loading (determined by mass balance via the Bradford method (in mg)) and, t is the reaction time (in min). Unless stated otherwise, the specific activity was determined after 20 hours of reaction.

$$Specific\ activity\ = \frac{nFAP\ converted}{t \times L}\ [U.mg^{-1}_{imm.\ TA}] \qquad \textbf{Eq. 3}$$

FAP and crystals solubility measurements

To measure the solubility of the FAP substrate and of the FMBA:DPPA crystals in the considered reaction media (HEPES 0.1 M pH 8 buffer containing PLP 1 mM and [0-20] % v/v of co-solvent), it is necessary to first create an oversaturated medium. Hence, saturated solutions were created by adding excess crystals or FAP, leading to the obtention of biphasic media (i.e. suspensions or emulsion). Afterwards, 100 µL of the saturated aqueous phase of the resulting mixtures were sampled (i.e. by filtrating suspensions (containing the FMBA:DPPA crystals) with 0.2 µm filter, or by exclusively pipetting the aqueous solution (containing the FAP substrate)), basified with 30 µL NaOH 2 M and then extracted using DCM (as described in the previous section), and analyzed by gas chromatography (see section 1 of the ESI).

2.5 Crystals characterization

After having been rinsed and filtered, the obtained crystals were analyzed and compared to reference crystals (namely, FMBA:DPPA ref and ISO:DPPA ref) which were chemically synthesized by 20 hours crystallization in Methyl Tert-Butyl Ether (MTBE) [36].

Proton Nuclear Magnetic Resonance (^{1}H-NMR)

Crystals were analyzed in ^{1}H-NMR in order to qualitatively assess their chemical composition and compare their spectrum with that of chemically produced reference crystals, and quantitatively via the use of an internal standard, namely, N,N-Dimethylformamide (DMF), allowing to measure their purity (in %), thereby attesting the validity of the whole process in the aim of API crystals production. More precisely, the FMBA:DPPA content of the crystals (x_{FMBA}) was determined by semi-quantitative ^{1}H-NMR analyses, by comparing the peak contributions of FMBA:DPPA (doublet 3H, at 1.57 ppm) and ISO:DPPA (doublet 6H, at 1.25 ppm) with each other (Eq. 4). DMF was used as standard for quantification during the ^{1}H-NMR analyses. Experimental details about ^{1}H-NMR analyses are provided in the first section of the ESI.

$$x_{FMBA}\,(\%) = \left(\frac{[FMBA{:}\,DPPA]}{[FMBA{:}\,DPPA] + [ISO{:}\,DPPA]}\right) * 100 \qquad \boldsymbol{Eq.4}$$

Powder X-ray Diffraction (pXRD)

The solid samples were analyzed via pXRD to assess their crystalline phases and characterize the solid composition of donor salt and/or product salt. Crystals were sprinkled on a sample holder coated with Nivea cream, which is then inserted in a Bruker-D8 Advance diffractometer with a Bragg-Brentano geometry. A copper anode under 40 kV and 30 mA produces the X-ray radiation with a Cu Kα wavelength (λ) of 1.54 Å. The Bruker detector was using a LynxEye XE-T technology and was recording intensities obtained with a 2θ value between 5° and 80° with 2θ increments of 0.015° and 0.15 seconds per step. The diffractograms obtained were analyzed with the DIFFRAC.EVA software (Bruker).

Chiral High Performance Liquid Chromatography (Chiral-HPLC)

Enantiomeric excess (ee) of FMBA was determined using Chiral High Performance Liquid Chromatography (Chiral-HPLC) and through chiral Gas Chromatography (cGC) analysis, by dissolving the obtained product crystals (FMBA:DPPA) in the mobile phases (see details in section 1 of the ESI).

Thermogravimetric analysis (TGA)

Crystals were analyzed by TGA) to assess their specific composition (e.g. water content) and thermal stability. Analyses were performed on a Mettler Toledo TGA-STDA 851e, from 25 to 400 °C, at a scanning rate of 10 °C·min^{-1}. The solid samples (5 to 10 mg) were placed in aluminium oxide crucibles. The purge gas was nitrogen, with a continuous flow rate of 50 mL·min^{-1}. Data were processed with the STARe 12.12 software.

3 Results and discussion

3.1 Catalytic performance of free and immobilized TAs (without product crystallization)

Two TA-loaded PP membranes (TA_PP and TA_PP_SS), were employed to run the asymmetric synthesis of (R)-2-fluoro-α-methylbenzylamine ((R)-FMBA). While TA_PP is obtained by immobilizing TsRTA on the functionalized PP membrane,[45] TA_PP_SS results from a simultaneous immobilization of TsRTA and PLP. This strategy was used in an attempt

to develop "self-sufficient" catalyst (i.e. no need for external addition of PLP during reaction [47]).

Owing to the configuration and dimensions of the batch reactors considered in this work, the amount of membrane employed per catalytic test was limited (i.e. 7 cm^2, which corresponds to c.a. 35 mg of flat-sheet membrane), resulting in very low TA loading in the reactor. Poor reaction rates were thus expected, given the low enzyme loading. The specific activities of both PP-immobilized TA were evaluated and compared to those of the soluble enzyme (free TsRTA) at identical enzyme loading/content (Figure 2, black triangles). We also compared their specific activities to those of other immobilized TAs, i.e. TsRTA immobilized on commercially available epoxy resins (TA_RelizymeEP) and amino-epoxy resins (TA_RelizymeHFA), used as conventional supports. In order to compare the catalytic performance of the different heterogeneous biocatalysts, the TA immobilizations (and subsequent transaminations) were run with identical masses of supports (i.e. 35 mg of functionalized PP membrane or Relizyme™ beads). It was observed that TA_RelizymeEP and TA_RelizymeHFA recovered 69 % and 84 % of specific activity (estimated using the first data point of the activity profiles shown in Figure S2 (i.e. 20 hours)) respectively, with respect to free TA. Such level of specific activity recoveries match with other reports on TAs immobilized on polymeric resins [48,49]. However, high TA loadings were observed on the Relizyme carriers (Figure 2, black triangles). These high TA immobilization yields recorded on the Relizyme carriers can easily be explained by the fact that resins display significantly higher surface area available to immobilize TAs, due to their smaller average pore diameters (i.e. 20 nm range) [26], with respect to the considered PP flat-sheet membranes (i.e. around 200 nm) [50]. However, the narrower pore diameter of the Relizymes may also bring additional restrictions (*e.g.* mass transport limitations, or highly constrained enzyme), which may partly explain the incomplete (< 100%) specific activity recoveries of those resin-immobilized biocatalysts. This aspect is even more pronounced at high enzyme loading since at some point, the increase of substrate consumption rate eventually surpasses the supply rate of substrate towards the immobilized enzyme [51].

On the other side, the specific activities exhibited by both PP-immobilized TAs were by far superior to those of the other biocatalysts tested herein (Figure 2). Normalized activities ($U.g_{cat}^{-1}$) and specific activities ($U.mg_{TA}^{-1}$) observed in this study compared well with the values obtained on other asymmetric syntheses (employing ISO as amine donor), as shown in Table S1 [49,52]. For example, the specific activities reported by Heckmann and Paradisi (towards the asymmetric synthesis of 2-aminobutane) [49] for two soluble cell-free extract TAs (*RTA-43 and

HeWT_F84W) are similar to the values obtained in this work (see Table S1, lower part). Notably, the specific activities displayed by TA_PP and TA_PP_SS catalysts correspond to specific activity recoveries of c.a. 340 % and 225 % with respect to free TA, respectively. These results notably highlight the robustness of the self-sufficient TA_PP_SS biocatalyst, which was able to efficiently catalyze such asymmetric synthesis of (R)-FMBA in absence of externally added co-factor. Expectedly (as observed in our previous work), its specific activity was lower than that of the "classical" immobilized transaminase (TA_PP), potentially due to the higher enzyme loading present on TA_PP_SS, which is likely to cause molecular crowding effect [27,53].

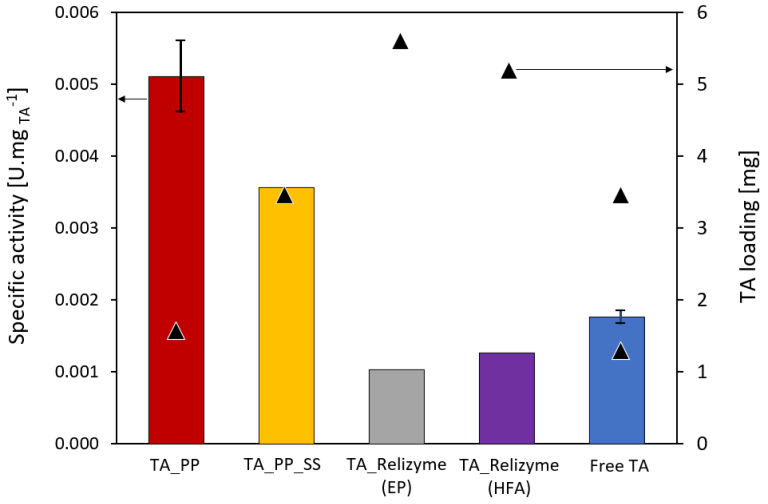

Figure 2. Immobilized TsRTA loading on solid biocatalysts (i.e. amount of enzymes immobilized on the carrier) or soluble enzyme concentration (triangles; 2 experiments designed as to have the same amount of enzyme as in TA_PP and TA_PP_SS), and specific activity (histograms) displayed by the different biocatalysts. TA_PP has been tested in triplicate. The error bar for the specific activity of Free TA is a combined standard deviation for the two experiments performed in triplicate for the free enzyme at different enzyme concentrations. Reaction conditions: 25 mM FAP, 250 mM ISO, 0 mM DPPA, 10 % v/v MeOH, 1 mM PLP (or 0 mM PLP for TA_PP_SS) in 0.1 M HEPES buffer pH 8, 35 °C.

The high specific activities of the PP-immobilized TAs and Free TA were also verified at an earlier stage of the reaction (6 hours) to avoid artifacts due to putative deactivation; this confirmed the superiority of the immobilized enzymes (Figure S3). Such high activity recoveries observed for TA_PP and TA_PP_SS may be attributed to the hydrophilic coating layers (PDA, and predominantly PEI) on the PP membranes, which stabilize the immobilized TAs by providing a suitable hydrated microenvironment. [54,55] In terms of overall activity (i.e. reaction rate, in [U]), the transamination reaction was faster when employing the membrane

immobilized TAs (Table S1, upper part), despite the significantly higher TA loadings obtained on both TA_Relizymes.

The activity dependence on FAP keto-substrate concentration was assessed for both soluble TA and TA_PP (Figure 3). 10 % v/v MeOH was used as co-solvent to ensure a proper dissolution of the substrate in the reaction medium. As expected, higher specific activities were observed when pure enzymes (pTAs; immobilized or soluble; see empty points in Figure 3) were employed. Noteworthily, for the free enzyme and TA_PP, the optimum FAP concentration was found to be around 10 mM and 25 mM, respectively, while enzyme inhibition by this keto substrate seemed to occur at higher concentrations. Such inhibition was particularly marked around 50 mM FAP, at which both the free and immobilized TA specific activities dropped by c.a. 50 % (with respect to their maximal values). It should be noted that TsRTA has previously been reported to run the asymmetric synthesis of the same (R)-FMBA up to 100 mM; yet this was measured at high enzyme concentration (i.e. 5 mg/mL) and with D-alanine as amino-donor [42].

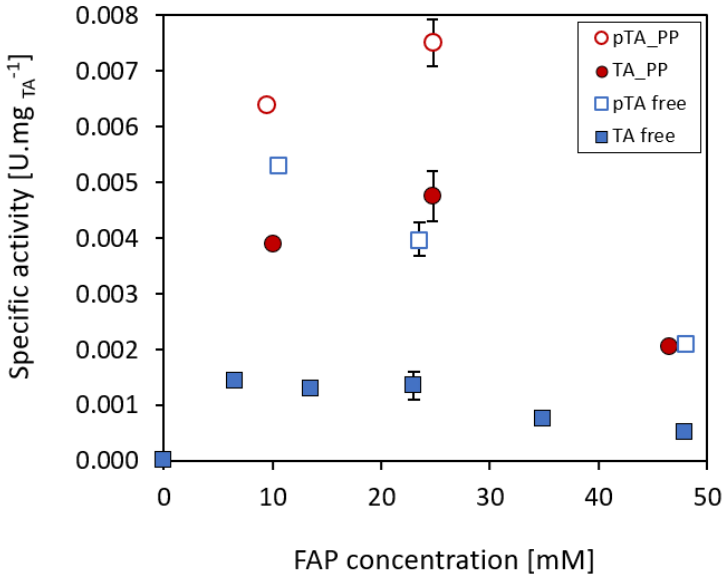

Figure 3. Specific activities obtained at different FAP initial concentrations, employing TA (TsRTA) cell-free extracts either soluble (blue squares) or immobilized as TA_PP (red dots), or purified TAs (pTAs) either soluble (empty squares) or immobilized as pTA_PP (red empty dots). Reaction conditions were: [6-48] mM FAP, 250 mM ISO, 0 mM DPPA, 10 % v/v MeOH, 1 mM PLP in 0.1 M HEPES buffer pH 8, 35 °C. All reactions were run at equal nominal enzyme concentration, i.e. 0.2 mg/mL TA. For (p)TA_PP, this corresponds to an enzyme loading of c.a. L ~ 1.5 mg (p)TA on the membrane carrier.

The long-term stability of the pTA_PP was investigated and compared to the one of soluble TA (at identical enzyme concentration/loading), by running the reaction and monitoring the

activity over time during extended durations. To this aim, 25 mM FAP with 10 molar equivalents of ISO (250 mM) were selected as standard reaction conditions. pTA_PP displayed remarkable activity and stability over time, whereas the soluble TAs were rapidly deactivated **(**Figure 4, full curves**)**. Such result is not surprising as it is often observed that the TA immobilization enhances the operational stability of the enzyme with respect to their free form [48]. When the FAP conversion began to stabilize (i.e. after 300 hours of reaction), the membrane (pTA_PP) was separated from the liquid reaction mixture, washed with HEPES 0.1 M, PLP 1 mM pH 8 buffer (three times) and immersed into a new reaction medium (prepared in identical conditions, i.e. 250 mM ISO, 25 mM FAP). Very similar specific activity was observed in such recyclability experiments, which allowed to ensure that the "activity plateau" observed in Figure 4a for pTA_PP was exclusively due to thermodynamic limitations (and not to enzyme deactivation; see Figure S4).

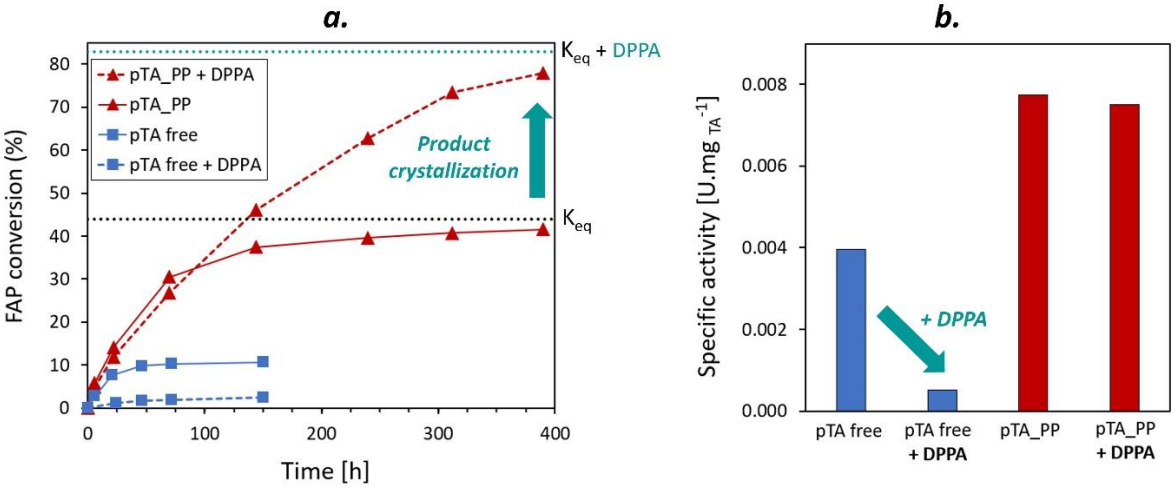

Figure 4. Catalytic performance (i.e. **a)** reaction profiles and **b)** specific activity) obtained with (50 mM) or without DPPA, employing pTAs either free (blue) or immobilized as pTA_PP (red). Reaction conditions were: 25 mM FAP, 250 mM ISO, 0 or 50 mM DPPA, 10 % v/v MeOH, 1 mM PLP in 0.1 M HEPES buffer pH 8, 35 °C. The reactions were run at equal nominal enzyme concentration, i.e. 0.2 mg/mL pTA. For pTA_PP, this corresponds to an enzyme loading of c.a. L ~ 1.5 mg TA on the membrane carrier.

The observed plateauing of FAP conversion leads to estimate the equilibrium conversion ($X_{FAP\ eq}$) to be ≈ 44 %. From this value, the transamination equilibrium constant was estimated to be $K_{eq} \approx 3.9 \times 10^{-2}$ (Figure S5), very close to the theoretical value computed using Gibbs free energies calculations ($K_{eq} = 4.7 \times 10^{-2}$, approximated by the MolCalc tool [56]), and with other studies estimating the K_{eq} value of model asymmetric syntheses (using ISO as amino-donor) [57].

All in all, these experiments confirmed that TA can be effectively immobilized on a PP membrane, and that the resulting biocatalyst is active, stable, and recyclable. The specific activity is higher than that of the free enzyme and yields close to the theoretical thermodynamic equilibrium can be achieved. Experiments have been carried out on small membrane discs featuring a low absolute amount of enzyme, which explains that long reaction times are needed. Yet, it is known that membranes can be packed in dense modules, which would solve the kinetic issue. Nevertheless, it appears pertinent to develop strategies to push the reaction towards completion by displacing the position of the thermodynamic equilibrium.

3.2 Crystallization-assisted transamination using membrane-immobilized TAs

pTA_PP was tested for the asymmetric synthesis of (R)-FMBA in presence of crystallizing agent DPPA, with the idea to push the transamination towards completion and to facilitate product separation and recovery. In order to maximize the product crystallization driving force, we performed the reaction in presence of an excess of DPPA (introduced above the solubility limit of the donor ISO:DPPA salt), in a *suspension-to-suspension* approach. This enables to keep the DPPA (and ISO) concentration constant over time (by progressive dissolution of the donor ISO:DPPA salt) [36].

The transamination-crystallization was run by modifying the standard conditions (25 mM FAP, 250 mM ISO) with the addition of 50 mM DPPA. In these precise conditions, the ISO and DPPA maximal soluble concentrations (i.e. dictated by the solubility product of the ISO:DPPA salt (K_{sp1} = 0.0036)) were estimated to 215 mM and 15 mM, respectively. By considering the FMBA solubility limit in the present system (s_{FMBA}), and by considering the estimated value of K_{eq}, it was possible to compute a new expected FAP conversion at the equilibrium obtained in presence of DPPA (green dotted line in Figure 4b). This corresponds to an expected equilibrium conversion of ~83% (much higher than the 44% limit in the case of the non-assisted reaction). However, in such conditions, the activity of free TA was dramatically affected (Figure 4b, dotted blue curve). Conversion was even lower than in the standard conditions (without DPPA). We tentatively ascribe such free enzyme deactivation to an undesired precipitation or immobilization of the soluble TsRTA on the ISO:DPPA crystals. Indeed, when running the reaction in the presence of only 15 mM of DPPA (i.e. below the solubility limit, and thus in the absence of solid crystals), the enzyme was barely affected (Figure S6). Further increasing the soluble enzyme concentration (from 0.2 mg/mL to 1 mg/mL pure TsRTA) did not change the activity profile obtained, as pronounced enzyme deactivation

was also observed (Figure S7). Interestingly, such free enzyme deactivation or precipitation induced by the presence of DPPA crystals was not observed when employing other TAs, such as HeWT (employing acetophenone as substrate, see Figure S7) or SpATA (employing 3-methoxy-acetophenone as substrate) [36], and appears thus to be an enzyme-dependent phenomenon.

On the contrary, running the crystallization-assisted reaction with the membrane immobilized TA (pTA_PP) allowed overcoming the initial equilibrium conversion (~44%), reaching as high as 77.4% conversion (Figure 4b, dotted red curve), approaching the theoretical limit of the crystallization-assisted process (~83%). Thus, immobilization is clearly identified as key to the success of this strategy. The impact of such FMBA:DPPA crystallization on pTA_PP specific activity, on final transamination yield and on the obtained crystals purity was investigated. By comparing the ^{1}H-NMR spectra of the obtained crystals with those of chemically synthesized donor (i.e. ISO:DPPA ref., Figure S8) and product (i.e. rac-FMBA:DPPA ref., Figure S9) crystal salts, we can estimate the relative amounts of FMBA:DPPA phase in the obtained crystals as well as the FMBA:DPPA crystals recovery yield (Table 1). In absence of product crystallization (i.e. without DPPA), the transamination is limited by its unfavorable thermodynamic equilibrium and only moderated yields can be obtained (Table 1, entries 1 and 4). Adding DPPA at the solubility limit (e.g. 15 mM) enabled the formation of the poorly soluble FMBA:DPPA crystal salt (Figure S10), which drove the transamination reaction towards higher FAP conversion as compared to the non-assisted reaction (Table 1, compare entry 2 to entry 1). Further increasing the total DPPA content from 15 mM to 50 mM (suspension containing ISO:DPPA donor crystal salt) enabled to achieve an even higher final substrate conversion, owing to the higher crystallization driving force (i.e. constant DPPA concentration over time). Noteworthily, performing the heterogeneous transamination in such suspension-to-suspension approach did not alter the specific activity of the membrane biocatalyst (i.e. the initial activity was unchanged). When employing low FAP substrate concentration (12.5 mM) with respect to the ISO:DPPA salt, the resulting crystals were not pure (i.e. contained only 62 % of FMBA:DPPA phase (and consequently, 38% of ISO:DPPA) see Figure S11 and Table 1, entry 3). Despite this aspect, high product crystal salt recovery was still obtained, resulting in 93 % overall FMBA:DPPA crystals recovery yield. Expectedly, doubling the FAP substrate concentration (to 25 mM) allowed to increase the proportion of FMBA:DPPA crystals in the collected solid (compare Table 1, entries 5 to 3), resulting in 97 % purity for the desired crystal phase (Figure S12) and 95 % crystals recovery

yield. These values correspond to an overall FMBA crystallization yield ($Y_{overall,}$ i.e. the proportion of FAP substrate ending up in the form of crystallized FMBA salt) of 72 %. We argue that such metrics are encouraging in the perspective of implementation for API production at the industrial scale [40]. It is noteworthy that the strategy can also be applied in the absence of externally added PLP. Using the "self-sufficient" membrane biocatalyst (TA_PP_SS) we reached similar yields of FMBA:DPPA crystals (Table S2).

Table 1. pTA_PP catalytic performance and crystallization metrics obtained when performing the transamination in presence of different DPPA and FAP contents). Reaction conditions were: [12.5-25] mM FAP, 250 mM ISO, [0-50] mM DPPA, 10 % v/v MeOH, 1 mM PLP in 0.1 M HEPES buffer pH 8, 35 °C. The enzyme loading was c.a. L ~ 1.5 mg pTA on the membrane carrier. The final FAP conversion was determined after 390 hours of reaction.

	Crystal name	C_0 FAP [mM]	Initial reaction medium	C DPPA [mM]	Sp. activity [U.mg$_{TA}^{-1}$] ([U. m^{-2}])	$X_{FAP\ eq}$ (%) [a]	$X_{FAP\ obs}$ (%) [b]	$x_{FMBA:DPPA}$ crystals (mol %) [c]	Y_{recov} FMBA:DPPA (%) [d]	$Y_{overall}$ FMBA:DPPA (%) [e]
1	/	12.5	Solution	0	0.0067 (16.9)	56.1	55.2	/	/	/
2	FMBA:DPPA (12.5:15)	12.5	Solution	15	0.0065 (16.5)	80.7	62.5	95	74 [d1]	44
3	FMBA:DPPA (12.5:50)	12.5	Suspension	50	0.0064 (16.3)	83.6	84.1	62	93 [d2]	48
4	/	25	Solution	0	0.0079 (21.7)	44.6	43.9	/	/	/
5	FMBA:DPPA (25:50)	25	Suspension	50	0.0075 (21.2)	81.9	77.5	97 ± 2 [f]	95 ± 3.2 [f]	72

[a]: Expected FAP conversion at the transamination equilibrium ($X_{FAP\ eq}$, see Eq. S4 and Eq. S5 in Supplementary informations of Chapter IV)

[b]: Observed FAP conversion after 390 hours of reaction

[c]: FMBA:DPPA content in the produced crystals ($x_{FMBA:DPPA}$, see Eq. 4)

[d]: FMBA:DPPA crystals recovery yield (Y_{recov} , see Eq. 3) ; the detailed calculation of d1 and d2 are reported in the ESI

[e] :FMBA:DPPA crystals overall yield, denoted $Y_{overall} = (Y_{recov} * x_{FMBA:DPPA} * X_{FAP\ obs})*100\%$

[f] :this experiment was reproduced three times (triplicate); mean values ± standard deviations are reported

Additionally, ^{1}H-NMR performed on the FMBA:DPPA (25:50) crystals (recovered from the experiment described in Table 1, entry 5) confirmed that the relative amounts of FMBA and DPPA species were 49:51. Thus, the crystal partners arrange in a 1:1 ratio to form the target FMBA:DPPA crystal structure. Thermogravimetric analysis (TGA) (Figure S13) further revealed only two distinct weight losses corresponding to FMBA (37.3 wt % (or 48.6 mol %), from c.a. 90 to 210 °C) and to DPPA (59.7 wt % (or 48.4 mol %), from c.a. 210 to 325 °C). The absence of minor low temperature weight losses shows that the crystals are not hydrates.

pXRD analyses revealed that crystals obtained *via* the transamination-crystallization approach displayed similar pXRD patterns as the chemically synthesized rac-FMBA:DPPA ref. crystals (Figure S14). However, when zooming in, several shifts in their pXRD peak positions were noticed (Figure S15). Given the high purity of the produced FMBA:DPPA (25:50) crystals (i.e. 99 mol % according to ^{1}H-NMR), such dissimilarity is probably induced by the fact that the crystals formed during the crystallization-assisted reaction should be enantiopure while those in rac-FMBA:DPPA ref. are racemic (as suggested by chiral GC (Figure S16) and chiral HPLC (Figure S17) analyses). This phenomenon was previously observed with other chiral organic crystals (e.g. 3-chloromandelic acid) [58,59]. Here, it can be interpreted that the racemic salt does not form a conglomerate, as the pXRD patterns of rac-FMBA:DPPA ref. do not perfectly match those from the enantiopure sample (FMBA:DPPA (25:50)). We tentatively ascribe the differences in pXRD patterns to the presence of a solid solution or a racemic compound crystal [60,61].

It is noteworthy that, even though chiral HPLC and GC provide convincing evidence that the product crystal is enantiopure, there is no unambiguous evidence about its stereochemistry. As the free TsRTA enzyme has shown perfect enantioselectivity towards the (R)-FMBA enantiomer in previous studies [42,44], we assume that the product was the (R)-enantiomer. In order to confirm this, we attempted to produce single crystals of (R)-FMBA:DPPA (using the biocatalytically produced crystals), but results remained ambiguous. For future studies, we advise choosing a model substrate (other than acetophenone, which is not accepted by the TsRTA enzyme) leading to a well-characterized crystal salt, as it would enable to overcome this problem.

The reusability of the membrane-immobilized TA in this crystallization-assisted transamination process was investigated. To this aim, the pTA_PP catalyst was employed to run three successive catalytic cycles in the presence of 50 mM DPPA. Each catalytic cycle was

stopped when the FAP conversion approached the conversion plateau. After each cycle, the membrane was removed from the resulting reaction mixture, rinsed three times with HEPES 0.1 M buffer pH 8, and then re-immersed into a fresh reaction medium. As observed in Figure 5, pTA_PP was able to perform high-yield successive (R)-FMBA asymmetric syntheses: final FAP conversions tending towards the expected conversion dictated by the transamination equilibrium in presence of FMBA:DPPA crystallization (i.e. $X_{FAP\ eq}$' ≈ 87 % in these conditions) were always observed. Of course, possible deactivation should be quantitatively assessed far away from the thermodynamic equilibrium [62]. pTA_PP was shown to retain 77 % of its initial specific activity after three transamination cycles (i.e. 1200 hours of operation). These results underline the robustness and the reusability of such membrane-immobilized TA.

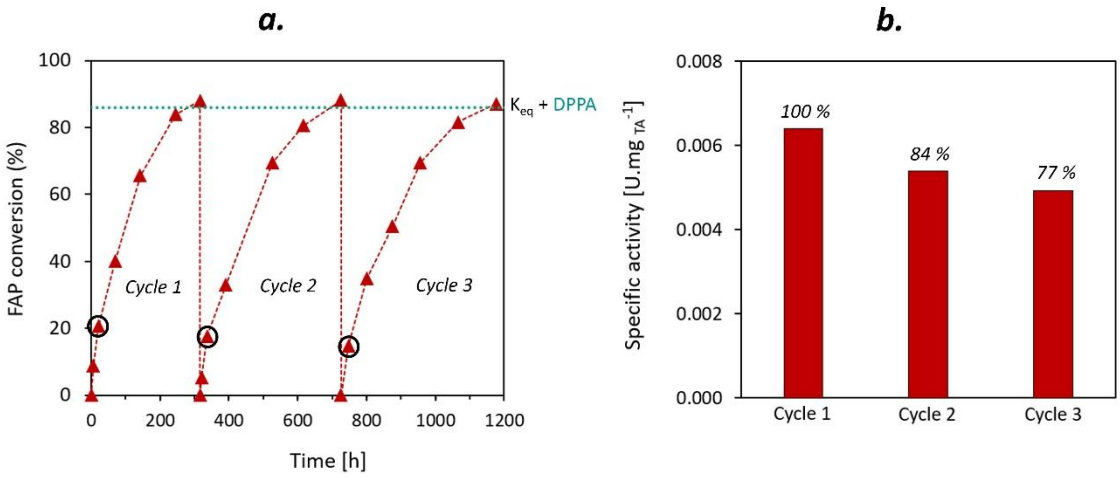

Figure 5. Recyclability tests (i.e. a) reaction profiles and b) specific activity) obtained when employing the pTA_PP catalyst. Reaction conditions were: 10 mM FAP, 250 mM ISO, 50 mM DPPA, 10 % v/v MeOH, 1 mM PLP in 0.1 M HEPES buffer pH 8, 35 °C. The enzyme loading was of c.a. L ~ 1.5 mg pTA on the membrane carrier.

Note that attempts to further enhance the process by using co-solvents (i.e. short-chain alcohols, DMF and ACN) that could potentially increase the solubility gap between the donor and product crystal salts (s_1 vs. s_2) were unsuccessfull (see ESI Fig. S18-21 and discussion therein).

On the contrary, ommitting methanol was found beneficial. Indeed, it should be noted that MeOH was initially employed as a way to ensure the complete solubility of the FAP substrate in the reaction medium. However, the ketone substrate is known to provoke enzyme inhibition. With 50 mM of FAP fully solubilized in the presence of MeOH, the specific activity dropped significantly as compared to 25 mM (Fig. 6a). A possible strategy to maintain good productivity

levels in batch mode is to take advantage of the low FAP solubility in aqueous media, as proposed by von Langermann et al [36]. FAP solubility in the aqueous reaction medium (without co-solvent) was estimated to s_{FAP} ~ 25 mM (Figure S21a). Thus, in absence of MeOH, if we introduce 50 mM of FAP, the actual concentration in the aqueous phase remains ~25 mM (and the excess is present as a separate liquid phase i.e. FAP emulsions, acting as external substrate reservoir). In such case, the TA_PP specific activity was fully maintained, and in fact slightly higher than that observed in presence of 25 mM of FAP (Figure 6a). Here, the FAP concentration (~25 mM, at which the enzyme is not inhibited) is maintained constant during reaction as long as the converted FAP is compensated by solubilization from the FAP reservoir. This strategy allowed to enhance the reaction kinetics by avoiding enzyme inhibition by FAP substrate, and feeding the process with constant substrate concentration. In principle, this configuration should allow to operate the crystallization-assisted transamination with any FAP sustrate concentration. For the proof-of-concenpt, the reaction was run in presence of 125 mM of FAP (Figure 6a): expectidly, the specific activity was maintained at the same level, which validated our hypothesis. It should be noted that the FMBA production profile showed a more pronounced linear trend (Figure 6b). The latter probably highlights a degenerescence of the kinetics ("pseudo zero-order" reaction), in which the reaction rate is constant over time due to the steady FAP substrate concentration present in the aqueous phase (s_{FAP}). Once the biocatalytic consumption overcomes the s_{FAP}, the biocatalytic reaction bounces back to a standard kinetic profile.

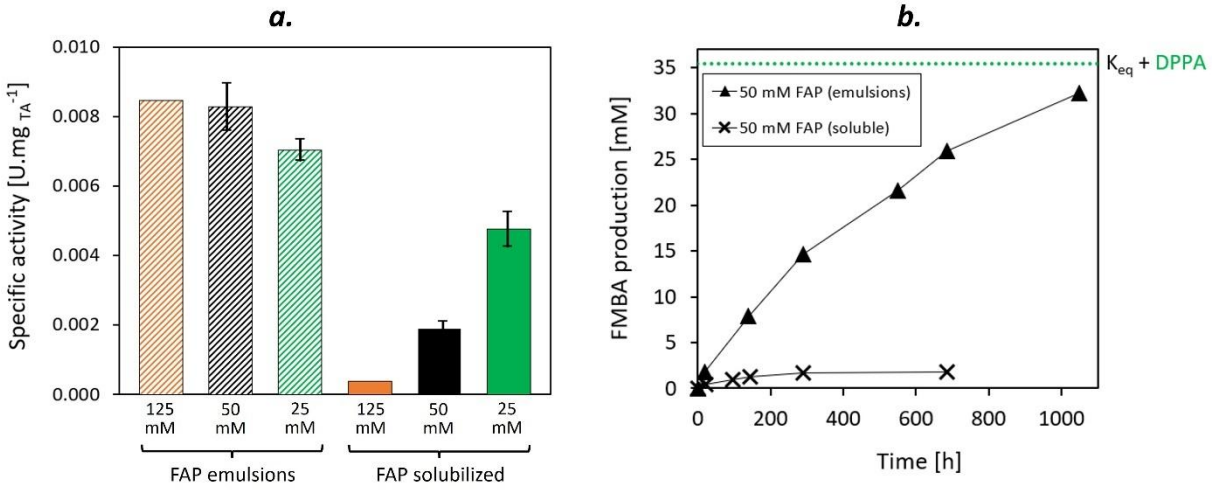

Figure 6. a) specific activity obtained (obtained at 20h) when employing TA_PP, using 25 mM (green), 50 mM (black) or 125 mM (orange) FAP substrate, in presence (full bars) or in absence (dashed bars) of MeOH (as co-solvent) in the reaction medium. Reaction conditions were: [25-125] mM FAP, 250 mM ISO, 50 mM DPPA, [0 or 10] % v/v MeOH (or [0 or 20] % v/v when 125 mM FAP was employed), 1 mM PLP in 0.1 M HEPES

buffer pH 8, 35 °C. The enzyme loading was of c.a. L ~ 1.5 mg TA on the membrane carrier. b) corresponding kinetic profiles obtained with 50 mM FAP in the presence (soluble) or absence (emulsion) of MeOH

3.3 Sustainability evaluation

To assess the sustainability of the studied crystallization-assisted transamination process, the E-factor of the lab-scale process was roughly estimated and compared to three chemocatalytic benchmark processes (Table 2). These benchmark methods A, B, and C for the synthesis of enantiopure α-methylbenzylamine derivatives are described in details in the ESI (Figure S22 to S24) [63]. The transamination process proposed in this work was found to feature significantly lower E-factor as compared to the benchmark chemocatalytic processes. Additionally, it must be emphasized that the biocatalytic strategy should produce enantiopure (F)MBA product (99.9 % ee, as suggested by chiral HPLC and GC analyses), which is not the case of the other chemocatalytic methods. In the latter, the presence of significant fractions of the other enantiomer imposes further purifications (e.g. preferential crystallizations), which is known to markedly impact the overall environmental and economic performance of such processes. [6,15] This underlines the superior performance of the crystallization-assisted biocatalytic route proposed herein.

Table 2. Comparison of environmental performance (E-factor) of the optimized crystallization-assisted asymmetric biocatalytic route (D) with different benchmark chemocatalytic routes (A, B, C) to chiral amines**.** S-methylbenzylamine (S-MBA) was the target amine in A and C, while (R)-FMBA was targeted in B and D.

Method (ref.)	**A ([64])**	**B ([65])**	**C ([66])**	**D (This work)**
Description	Imine asymmetric hydrogenation	Ketone reductive amination	Chiral resolution + crystallization	Transamination + crystallization
Precursors	Imine, H_2	Ketone, H_2, NH_4OAc	Racemic amine + resolv. agent [a]	Ketone, ISO + DPPA
Talyst	$[Rh(COD)Cl]_2$-(Ligand)	$Ru(OAc)_2$-(Ligand)	/	TA_PP, PLP
ee (%)	90	95	69	99.9 [b]
E-factor	58	18	19	5 (or 2.6 *) [c]

[a] : N-tosyl-(S)-phenylalanine (S-TPA) was used as resolving agent.

[b] : only one peak was detected in the chiral GC and HPLC analyses

[c] :Reaction conditions were: 50 mM FAP, 250 mM ISO, 50 mM DPPA, 1 mM PLP in 0.1 M (or 0.05 M *) HEPES buffer pH 8, 35 °C.

4 Conclusion

In this work, we present the immobilization of a R-selective TA (TsRTA) onto a porous polypropylene membrane (PP) and its application to catalyze an industrially relevant transamination: the asymmetric synthesis of (R)-2-fluoro-α-methylbenzylamine ((R)-FMBA). To boost the reaction and reach high product yields, product separation was achieved by in situ crystallization.

PP was coated with polydopamine to provide amine functions at its surface, which were further functionalized with epoxy groups to covalently graft the TA. The immobilized TA showed enhanced specific activity and stability towards the studied transamination compared to their soluble counterparts. It also exhibited superior catalytic performance than widely employed heterogeneous TAs (i.e. Relizyme™-immobilized TAs). Crystallization of (R)-FMBA with 3,3-diphenylpropionic acid (DPPA) was shown to displace the transamination equilibrium towards the product side. Also, the targeted enantiopure amine was recovered by simple filtration (in the form of a high purity salt). The overall yield reached 72 % of the substrate FAP recovered in the form of (R)-FMBA:DPPA crystals (which has to be compared to ~40% conversion in soluble form for the non-assisted process). The PP-immobilized TA was shown to be easily recoverable and reusable, being able to perform successive high-yield asymmetric syntheses with minor deactivation. Also, working in the absence of co-solvent resulted in the formation of an FAP emulsions, and in a low (c.a. 25 mM) but constant concentration of soluble FAP (the emulsion playing the role of an FAP reservoir). This configuration allowed engaging higher amounts of the keto-substrate concentrations while minimizing enzyme inhibition and boosting productivity. Overall, the method presented herein could pave the way to the use of membrane-supported enzymes in hybrid processes, i.e. concatenated with membrane-assisted purification strategies.

5 Acknowledgments

This work was funded by Actions de Recherche Concertée (ARC) under the project « PURE » (20/25-108) and by the Fonds de la Recherche Scientifique (FNRS) under the project CDR J.0044.20. The chiral HPLC analyses were performed by Laurent Collard. We than Dr. Cédric Gastaldi and Ir. Aurélien Doutry for having performed ^{1}H_NMR analyses. Dr. François Devred is thanked for the logistic support.

6 Supporting Information

Supporting Information: Experimental details on protocols and analytical methods (PP membrane functionalization, Soluble enzyme quantification, GC, chiral GC and chiral HPLC analysis methodologies, ^{1}H-NMR analysis methodologies) and Supplementary Figure and Discussion Points (Theoretical calculations on the crystallization yields and conversion at the equilibrium, Attempts to further push the crystallization-assisted transamination reaction by adding co-solvents, Sustainability metrics (E-factor) evaluation)

7 References

(1) D. Patil, M.; Grogan, G.; Bommarius, A.; Yun, H. Recent Advances in ω-Transaminase-Mediated Biocatalysis for the Enantioselective Synthesis of Chiral Amines. *Catalysts* **2018**, *8* (7), 254.

(2) Ghislieri, D.; Turner, N. J. Biocatalytic Approaches to the Synthesis of Enantiomerically Pure Chiral Amines. *Top. Catal.* **2014**, *57* (5), 284–300.

(3) Arango, H. M.; Biggelaar, L. van den; Soumillion, P.; Luis, P.; Leyssens, T.; Paradisi, F.; Debecker, D. P. Continuous Flow-Mode Synthesis of (Chiral) Amines with Transaminase: A Strategic Biocatalytic Approach to Essential Building Blocks. *React. Chem. Eng.* **2023**, *8* (7), 1505–1544. https://doi.org/10.1039/D3RE00210A.

(4) Anastas, P. T.; Warner, J. C. *Green Chemistry: Theory and Practice*; Oxford University Press: New York, 1998; Vol. 2.

(5) Debecker, D. P.; Kuok (Mimi) Hii, K.; Moores, A.; Rossi, L. M.; Sels, B.; Allen, D. T.; Subramaniam, B. Shaping Effective Practices for Incorporating Sustainability Assessment in Manuscripts Submitted to ACS Sustainable Chemistry & Engineering: Catalysis and Catalytic Processes. *ACS Sustain. Chem. Eng.* **2021**, *9* (14), 4936–4940. https://doi.org/10.1021/acssuschemeng.1c02070.

(6) Savile, C. K.; Janey, J. M.; Mundorff, E. C.; Moore, J. C.; Tam, S.; Jarvis, W. R.; Colbeck, J. C.; Krebber, A.; Fleitz, F. J.; Brands, J.; Devine, P. N.; Huisman, G. W.; Hughes, G. J. Biocatalytic Asymmetric Synthesis of Chiral Amines from Ketones Applied to Sitagliptin Manufacture. *Science* **2010**, *329* (5989), 305–309.

(7) Slabu, I.; Galman, J. L.; Lloyd, R. C.; Turner, N. J. Discovery, Engineering, and Synthetic Application of Transaminase Biocatalysts. *ACS Catal.* **2017**, *7* (12), 8263–8284.

(8) Guo, F.; Berglund, P. Transaminase Biocatalysis: Optimization and Application. *Green Chem.* **2017**, *19* (2), 333–360.

(9) Ferrandi, E. E.; Monti, D. Amine Transaminases in Chiral Amines Synthesis: Recent Advances and Challenges. *World J. Microbiol. Biotechnol.* **2017**, *34* (1), 13.

(10) Wallace, D. J.; Mangion, I.; Coleman, P. Discovery and Chemical Development of Suvorexant - A Dual Orexin Antagonist for Sleep Disorder. In *Comprehensive Accounts of Pharmaceutical Research and Development: From Discovery to Late-Stage Process Development Volume 1*; ACS Symposium Series; American Chemical Society, 2016; Vol. 1239, pp 1–36.

(11) Girardin, M.; Ouellet, S. G.; Gauvreau, D.; Moore, J. C.; Hughes, G.; Devine, P. N.; O'Shea, P. D.; Campeau, L.-C. Convergent Kilogram-Scale Synthesis of Dual Orexin Receptor Antagonist. *Org. Process Res. Dev.* **2013**, *17* (1), 61–68.

(12) Novick, S. J.; Dellas, N.; Garcia, R.; Ching, C.; Bautista, A.; Homan, D.; Alvizo, O.; Entwistle, D.; Kleinbeck, F.; Schlama, T.; Ruch, T. Engineering an Amine Transaminase for the Efficient Production of a Chiral Sacubitril Precursor. *ACS Catal.* **2021**, *11* (6), 3762–3770.

(13) Chung, C. K.; Bulger, P. G.; Kosjek, B.; Belyk, K. M.; Rivera, N.; Scott, M. E.; Humphrey, G. R.; Limanto, J.; Bachert, D. C.; Emerson, K. M. Process Development of C–N Cross-Coupling and Enantioselective Biocatalytic Reactions for the Asymmetric Synthesis of Niraparib. *Org. Process Res. Dev.* **2014**, *18* (1), 215–227.

(14) Burns, M.; Martinez, C. A.; Vanderplas, B.; Wisdom, R.; Yu, S.; Singer, R. A. A Chemoenzymatic Route to Chiral Intermediates Used in the Multikilogram Synthesis of a Gamma Secretase Inhibitor. *Org. Process Res. Dev.* **2017**, *21* (6), 871–877.

(15) Yang, J.; Buekenhoudt, A.; Dael, M. V.; Luis, P.; Satyawali, Y.; Malina, R.; Lizin, S. A Techno-Economic Assessment of a Biocatalytic Chiral Amine Production Process Integrated with In Situ Membrane Extraction. *Org. Process Res. Dev.* **2022**, *26* (7), 2052–2066. https://doi.org/10.1021/acs.oprd.1c00464.

(16) Gomm, A.; O'Reilly, E. Transaminases for Chiral Amine Synthesis. *Curr. Opin. Chem. Biol.* **2018**, *43*, 106–112.

(17) Tamborini, L.; Fernandes, P.; Paradisi, F.; Molinari, F. Flow Bioreactors as Complementary Tools for Biocatalytic Process Intensification. *Trends Biotechnol.* **2018**, *36* (1), 73–88.

(18) Benítez-Mateos, A. I.; Contente, M. L.; Padrosa, D. R.; Paradisi, F. Flow Biocatalysis 101: Design, Development and Applications. *React. Chem. Eng.* **2021**, *6* (4), 599–611.

(19) Romero-Fernández, M.; Paradisi, F. Protein Immobilization Technology for Flow Biocatalysis. *Curr. Opin. Chem. Biol.* **2020**, *55*, 1–8.

(20) Gérardy, R.; Debecker, D. P.; Estager, J.; Luis, P.; Monbaliu, J.-C. M. Continuous Flow Upgrading of Selected C2–C6 Platform Chemicals Derived from Biomass. *Chem. Rev.* **2020**, *120* (15), 7219–7347.

(21) G. Newman, S.; F. Jensen, K. The Role of Flow in Green Chemistry and Engineering. *Green Chem.* **2013**, *15* (6), 1456–1472. https://doi.org/10.1039/C3GC40374B.

(22) van den Biggelaar, L.; Soumillion, P.; Debecker, D. P. Biocatalytic Transamination in a Monolithic Flow Reactor: Improving Enzyme Grafting for Enhanced Performance. *RSC Adv.* **2019**, *9* (32), 18538–18546.

(23) Noriega-Hevia, G.; Serralta, J.; Seco, A.; Ferrer, J. Economic Analysis of the Scale-up and Implantation of a Hollow Fibre Membrane Contactor Plant for Nitrogen Recovery in a Full-Scale Wastewater Treatment Plant. *Sep. Purif. Technol.* **2021**, *275*, 119128. https://doi.org/10.1016/j.seppur.2021.119128.

(24) Verrecht, B.; Maere, T.; Nopens, I.; Brepols, C.; Judd, S. The Cost of a Large-Scale Hollow Fibre MBR. *Water Res.* **2010**, *44* (18), 5274–5283. https://doi.org/10.1016/j.watres.2010.06.054.

(25) Kahar, U. M.; Sani, M. H.; Chan, K.-G.; Goh, K. M. Immobilization of α-Amylase from Anoxybacillus Sp. SK3-4 on ReliZyme and Immobead Supports. *Molecules* **2016**, *21* (9), 1196. https://doi.org/10.3390/molecules21091196.

(26) *Resindion srl*. https://www.resindion.com/relizyme.php?content=technical-information (accessed 2024-01-03).

(27) Jochems, P.; Satyawali, Y.; Diels, L.; Dejonghe, W. Enzyme Immobilization on/in Polymeric Membranes: Status, Challenges and Perspectives in Biocatalytic Membrane Reactors (BMRs). *Green Chem.* **2011**, *13* (7), 1609–1623. https://doi.org/10.1039/C1GC15178A.

(28) Montanari, U.; Cocchi, D.; Brugo, T. M.; Pollicino, A.; Taresco, V.; Romero Fernandez, M.; Moore, J. C.; Sagnelli, D.; Paradisi, F.; Zucchelli, A.; Howdle, S. M.; Gualandi, C. Functionalisable Epoxy-Rich Electrospun Fibres Based on Renewable Terpene for Multi-Purpose Applications. *Polymers* **2021**, *13* (11), 1804. https://doi.org/10.3390/polym13111804.

(29) Shin, J. S.; Kim, B. G.; Liese, A.; Wandrey, C. Kinetic Resolution of Chiral Amines with Omega-Transaminase Using an Enzyme-Membrane Reactor. *Biotechnol. Bioeng.* **2001**, *73* (3), 179–187.

(30) Shin, J.-S.; Kim, B.-G. Kinetic Resolution of α-Methylbenzylamine with ω-Transaminase Screened from Soil Microorganisms: Application of a Biphasic System to Overcome Product Inhibition. *Biotechnol. Bioeng.* **1997**, *55* (2), 348–358.

(31) Rehn, G.; Adlercreutz, P.; Grey, C. Supported Liquid Membrane as a Novel Tool for Driving the Equilibrium of ω-Transaminase Catalyzed Asymmetric Synthesis. *J. Biotechnol.* **2014**, *179*, 50–55.

(32) Satyawali, Y.; Del Pozo, D. F.; Vandezande, P.; Nopens, I.; Dejonghe, W. Investigating Pervaporation for In Situ Acetone Removal as Process Intensification Tool in ω-Transaminase Catalyzed Chiral Amine Synthesis. *Biotechnol. Prog.* **2019**, *35* (1), e2731. https://doi.org/10.1002/btpr.2731.

(33) Hülsewede, D.; Temmel, E.; Kumm, P.; von Langermann, J. Concept Study for an Integrated Reactor-Crystallizer Process for the Continuous Biocatalytic Synthesis of (S)-1-(3-Methoxyphenyl)Ethylamine. *Crystals* **2020**, *10* (5), 345. https://doi.org/10.3390/cryst10050345.

(34) Hülsewede, D.; Tänzler, M.; Süss, P.; Mildner, A.; Menyes, U.; von Langermann, J. Development of an in Situ-Product Crystallization (ISPC)-Concept to Shift the Reaction Equilibria of Selected Amine Transaminase-Catalyzed Reactions. *Eur. J. Org. Chem.* **2018**, *2018* (18), 2130–2133. https://doi.org/10.1002/ejoc.201800323.

(35) Frodsham, L.; Golden, M.; Hard, S.; Kenworthy, M. N.; Klauber, D. J.; Leslie, K.; Macleod, C.; Meadows, R. E.; Mulholland, K. R.; Reilly, J.; Squire, C.; Tomasi, S.; Watt, D.; Wells, A. S. Use of ω-Transaminase Enzyme Chemistry in the Synthesis of a JAK2 Kinase Inhibitor. *Org. Process Res. Dev.* **2013**, *17* (9), 1123–1130.

(36) Neuburger, J.; Helmholz, F.; Tiedemann, S.; Lehmann, P.; Süss, P.; Menyes, U.; von Langermann, J. Implementation and Scale-up of a Semi-Continuous Transaminase-Catalyzed Reactive Crystallization for the Preparation of (S)-(3-Methoxyphenyl)Ethylamine. *Chem. Eng. Process. - Process Intensif.* **2021**, *168*, 108578. https://doi.org/10.1016/j.cep.2021.108578.

(37) Doeker, M.; Grabowski, L.; Rother, D.; Jupke, A. In Situ Reactive Extraction with Oleic Acid for Process Intensification in Amine Transaminase Catalyzed Reactions. *Green Chem.* **2022**, *24* (1), 295–304. https://doi.org/10.1039/D1GC03289E.

(38) Harmsen, B.; Leyssens, T. Enabling Enantiopurity: Combining Racemization and Dual-Drug Co-Crystal Resolution. *Cryst. Growth Des.* **2018**, *18* (6), 3654–3660. https://doi.org/10.1021/acs.cgd.8b00438.

(39) Dunn, A. S.; Svoboda, V.; Sefcik, J.; ter Horst, J. H. Resolution Control in a Continuous Preferential Crystallization Process. *Org. Process Res. Dev.* **2019**, *23* (9), 2031–2041. https://doi.org/10.1021/acs.oprd.9b00275.

(40) Brown, C.; McGlone, T.; Florence, A. Continuous Crystallisation. In *Continuous Manufacturing of Pharmaceuticals*; John Wiley & Sons, Ltd, 2017; pp 169–226. https://doi.org/10.1002/9781119001348.ch5.

(41) Tiedemann, S.; Neuburger, J. E.; Gazizova, A.; von Langermann, J. Continuous Preparative Application of Amine Transaminase-Catalyzed Reactions with Integrated Crystallization. *Eur. J. Org. Chem.* **2024**, *27* (13), e202400068. https://doi.org/10.1002/ejoc.202400068.

(42) Heckmann, C. M.; Paradisi, F. GPhos Ligand Enables Production of Chiral N-Arylamines in a Telescoped Transaminase-Buchwald-Hartwig Amination Cascade in the Presence of Excess Amine Donor. *Chem. – Eur. J.* **2021**, *27* (67), 16616–16620. https://doi.org/10.1002/chem.202103472.

(43) Cerioli, L.; Planchestainer, M.; Cassidy, J.; Tessaro, D.; Paradisi, F. Characterization of a Novel Amine Transaminase from Halomonas Elongata. *J. Mol. Catal. B Enzym.* **2015**, *120*, 141–150.

(44) Heckmann, C. M.; Gourlay, L. J.; Dominguez, B.; Paradisi, F. An (R)-Selective Transaminase From Thermomyces Stellatus: Stabilizing the Tetrameric Form. *Front. Bioeng. Biotechnol.* **2020**, *8*, 707.

(45) Arango, H. M.; Nguyen, X. D. L.; Luis, P.; Leyssens, T.; Padrosa, D. R.; Paradisi, F.; Debecker, D. P. Membrane-Immobilized Transaminases for the Synthesis of Enantiopure Amines. *RSC Sustain.* **2024**, *2* (10), 3139–3152. https://doi.org/10.1039/D4SU00293H.

(46) Benítez-Mateos, A. I.; Contente, M. L.; Velasco-Lozano, S.; Paradisi, F.; López-Gallego, F. Self-Sufficient Flow-Biocatalysis by Coimmobilization of Pyridoxal 5′-Phosphate and ω-Transaminases onto Porous Carriers. *ACS Sustain. Chem. Eng.* **2018**, *6* (10), 13151–13159.

(47) Reus, B.; Damian, M.; Mutti, F. G. Advances in Cofactor Immobilization for Enhanced Continuous-Flow Biocatalysis. *J. Flow Chem.* **2024**. https://doi.org/10.1007/s41981-024-00315-2.

(48) Planchestainer, M.; Contente, M. L.; Cassidy, J.; Molinari, F.; Tamborini, L.; Paradisi, F. Continuous Flow Biocatalysis: Production and in-Line Purification of Amines by Immobilised Transaminase from Halomonas Elongata. *Green Chem.* **2017**, *19* (2), 372–375.

(49) Heckmann, C. M.; Dominguez, B.; Paradisi, F. Enantio-Complementary Continuous-Flow Synthesis of 2-Aminobutane Using Covalently Immobilized Transaminases. *ACS Sustain. Chem. Eng.* **2021**, *9* (11), 4122–4129.

(50) Chergaoui, S.; Lauzer, J.; Debecker, D. P.; Leyssens, T.; Luis, P. Tuning Membrane Properties to Control Supersaturation of Antisolvent Crystallization. *J. Membr. Sci.* **2024**, *694*, 122415. https://doi.org/10.1016/j.memsci.2024.122415.

(51) Liese, A.; Hilterhaus, L. Evaluation of Immobilized Enzymes for Industrial Applications. *Chem. Soc. Rev.* **2013**, *42* (15), 6236–6249. https://doi.org/10.1039/C3CS35511J.

(52) Wang, X.; Xie, Y.; Wang, Z.; Zhang, K.; Wang, H.; Wei, D. Efficient Synthesis of (S)-1-Boc-3-Aminopiperidine in a Continuous Flow System Using ω-Transaminase-Immobilized Amino-Ethylenediamine-Modified Epoxide Supports. *Org. Process Res. Dev.* **2022**, *26* (5), 1351–1359. https://doi.org/10.1021/acs.oprd.1c00217.

(53) Bhattacharyya, D. Activity Studies of Immobilized Subtilisin on Functionalized Pure Cellulose-Based Membranes. *Biotechnol. Prog.* **2001**.

(54) Vander Straeten, A.; Lefèvre, D.; Demoustier-Champagne, S.; Dupont-Gillain, C. Protein-Based Polyelectrolyte Multilayers. *Adv. Colloid Interface Sci.* **2020**, *280*, 102161. https://doi.org/10.1016/j.cis.2020.102161.

(55) Velasco-Lozano, S.; Jackson, E.; Ripoll, M.; López-Gallego, F.; Betancor, L. Stabilization of ω-Transaminase from Pseudomonas Fluorescens by Immobilization Techniques. *Int. J. Biol. Macromol.* **2020**, *164*, 4318–4328. https://doi.org/10.1016/j.ijbiomac.2020.09.003.

(56) *MolCalc*. http://molcalc.org/ (accessed 2024-03-29).

(57) Tufvesson, P.; Jensen, J. S.; Kroutil, W.; Woodley, J. M. Experimental Determination of Thermodynamic Equilibrium in Biocatalytic Transamination. *Biotechnol. Bioeng.* **2012**, *109* (8), 2159–2162. https://doi.org/10.1002/bit.24472.

(58) Minh, T. L.; Langermann, J. V.; Lorenz, H.; Seidel-Morgenstern, A. Enantiomeric 3-Chloromandelic Acid System: Binary Melting Point Phase Diagram, Ternary Solubility Phase Diagrams and Polymorphism. *J. Pharm. Sci.* **2010**, *99* (9), 4084–4095. https://doi.org/10.1002/jps.22234.

(59) Hylton, R. K.; Tizzard, G. J.; Threlfall, T. L.; Ellis, A. L.; Coles, S. J.; Seaton, C. C.; Schulze, E.; Lorenz, H.; Seidel-Morgenstern, A.; Stein, M.; Price, S. L. Are the Crystal Structures of Enantiopure and Racemic Mandelic Acids Determined by Kinetics or Thermodynamics? *J. Am. Chem. Soc.* **2015**, *137* (34), 11095–11104. https://doi.org/10.1021/jacs.5b05938.

(60) Datta, S.; Grant, D. J. W. Crystal Structures of Drugs: Advances in Determination, Prediction and Engineering. *Nat. Rev. Drug Discov.* **2004**, *3* (1), 42–57. https://doi.org/10.1038/nrd1280.

(61) Diniz, L. F.; Carvalho, P. S. Jr.; da Nova Mussel, W.; Yoshida, M. I.; Diniz, R.; Fernandes, C. Racemic Salts and Solid Solutions of Enantiomers of the Antihypertensive Drug Carvedilol. *Cryst. Growth Des.* **2019**, *19* (8), 4498–4509. https://doi.org/10.1021/acs.cgd.9b00263.

(62) Schüth, F.; Ward, M. D.; Buriak, J. M. Common Pitfalls of Catalysis Manuscripts Submitted to Chemistry of Materials. *Chem. Mater.* **2018**, *30* (11), 3599–3600. https://doi.org/10.1021/acs.chemmater.8b01831.

(63) Yin, Q.; Shi, Y.; Wang, J.; Zhang, X. Direct Catalytic Asymmetric Synthesis of α-Chiral Primary Amines. *Chem. Soc. Rev.* **2020**, *49* (17), 6141–6153. https://doi.org/10.1039/C9CS00921C.

(64) Zhao, Q.; Wen, J.; Tan, R.; Huang, K.; Metola, P.; Wang, R.; Anslyn, E. V.; Zhang, X. Rhodium Catalyzed Asymmetric Hydrogenation of Unprotected N-H Imines Assisted by Thiourea. *Angew. Chem. Int. Ed Engl.* **2014**, *53* (32), 8467–8470. https://doi.org/10.1002/anie.201404570.

(65) Tan, X.; Gao, S.; Zeng, W.; Xin, S.; Yin, Q.; Zhang, X. Asymmetric Synthesis of Chiral Primary Amines by Ruthenium-Catalyzed Direct Reductive Amination of Alkyl Aryl Ketones with Ammonium Salts and Molecular H2. *J. Am. Chem. Soc.* **2018**, *140* (6), 2024–2027. https://doi.org/10.1021/jacs.7b12898.

(66) Hirose, T.; Begum, M.; Sadequl Islam, Md.; Taniguchi, K.; Yasutake, M. Resolution of α-Methylbenzylamine via Diastereomeric Salt Formation Using the Naturally Based Reagent *N*-Tosyl-(*S*)-Phenylalanine Together with a Solvent Switch Technique. *Tetrahedron Asymmetry* **2008**, *19* (14), 1641–1646. https://doi.org/10.1016/j.tetasy.2008.06.035.

For Table of Contents Only